

# Determination of the Donor Pair Exchange Energy in Phosphorus-Doped Silicon\*

P. R. CULLIS† AND J. R. MARKO

*Department of Physics, University of British Columbia, Vancouver, British Columbia*

(Received 9 January 1969; revised manuscript received 14 July 1969)

The EPR spectrum for relatively dilute samples of phosphorus-doped silicon ( $<5 \times 10^{16}$  donors/cm<sup>3</sup>) has been calculated in detail for an assumed random distribution of impurities. The system of donor electron spins is treated as a collection of nearest-neighbor donor pairs. An expression is derived for the donor pair exchange energy using Kohn-Luttinger wave functions and a general exchange-energy expression. The resultant relationship contains an adjustable parameter  $a^*$ , the "effective Bohr radius," which is determined from a comparison of the calculated spectrum and the experimental results obtained for the ratio  $C$  of the central-pair and hyperfine line intensities. The resulting expression  $J(\mathbf{R})$ , where  $J$  represents the exchange energy and  $\mathbf{R}$  the separation vector connecting the two pair donors, exhibits an oscillatory spatial dependence due to interference from portions of the wave function arising from different conduction-band valleys. The distribution of pair exchange energies is compared with earlier experimental determinations of this distribution.

## I. INTRODUCTION

THE electron-paramagnetic-resonance (EPR) spectrum of pairs of neighboring donor atoms in semiconductors was first considered by Slichter.<sup>1</sup> In that work, the line occurring midway between the two donor hyperfine lines in phosphorus-doped silicon was attributed to such pairs. This line was called the central-pair line because it was flanked by weaker components, also due to pairs, whose transition energies were identical to those of the more numerous isolated donors. In more concentrated samples, additional lines were found corresponding to transitions in clusters of three and four nearby donors.<sup>2</sup> Recently, one of us<sup>3</sup> extended these calculations to pairs for which the exchange energy  $J$  is on the order of the hyperfine interaction energy  $A$ . The results showed the presence of new lines outside the usual hyperfine lines as well as a splitting of the central-pair line. When the distribution of  $J$  values due to the random spacing of impurities was considered, these pairs were found to be a most likely source of a previously observed broad background line and related effects.<sup>2,4,5</sup>

This present work utilized a general calculation of the EPR spectrum of phosphorus-doped silicon as a function of  $J$  and an assumed random impurity distribution to determine the relationship  $J(\mathbf{R})$  between the exchange energy and the spatial separation vector  $\mathbf{R}$  between the members of a pair. A general expression is derived for  $J(\mathbf{R})$  in a calculation which does not explicitly include the effective-mass anisotropy of the silicon conduction bands. This neglect necessitates the introduction of a quantity  $a^*$ , the "effective Bohr

radius," the value of which is determined by a comparison of the calculated and experimental spectrum. This result is then compared with previous determinations and its significance to other experiments is discussed.

## II. CALCULATION OF EPR SPECTRUM

The spin Hamiltonian for a pair of donor atoms can be written

$$\mathcal{H} = g\mu_B H_0 (S_{1z} + S_{2z}) + A(\mathbf{I}_1 \cdot \mathbf{S}_1 + \mathbf{I}_2 \cdot \mathbf{S}_2) + J(\mathbf{S}_1 \cdot \mathbf{S}_2), \quad (1)$$

where  $I$  and  $S$  represent the nuclear and electronic spins, respectively ( $I = S = \frac{1}{2}$  for phosphorus donors),  $J$  is the exchange constant of the pair,  $A$  is the hyperfine constant,  $g$  is the electronic  $g$  value,  $\mu_B$  is the Bohr magneton, and  $H_0$  is the dc magnetic field. This expression neglects the very small Zeeman interaction of the nuclear spins with the field  $H_0$ . In the case where  $J \gg A$ , a total electronic spin  $\mathbf{S} = \mathbf{S}_1 + \mathbf{S}_2$  may be defined which enables Eq. (1) to be written as

$$\mathcal{H}_{\text{diag}} = g\mu_B H_0 S_z + \frac{1}{2} A S_z (m_1 + m_2) + \frac{1}{2} J (S^2 - \frac{3}{2}), \quad (2)$$

where  $S_z$  is the  $z$  component of the total electronic spin and  $m_i$  is the  $z$  component of the  $i$ th donor nucleus spin. In this expression, we have dropped all terms of the hyperfine interaction which are off diagonal in a representation which has, as its basis, the direct product of the eigenstates of the  $z$  component of the individual nuclear and electronic spins. This simplification is valid in our case because the inequality  $|g\mu_B H_0 \pm J| \gg A$ , which holds for essentially all donor pairs, guarantees a negligible (for our purposes) mixing of states through the perturbations introduced by these off-diagonal elements. The eigenstates of the operator in (2) are similarly the direct product of these nuclear spin eigenstates with the well-known singlet and triplet electronic spin states of the pair. These electronic spin states are analogous to those of the hydrogen molecule which arise from the coupling of the two spin- $\frac{1}{2}$  electrons into three states of total spin  $S=1$  and a single  $S=0$  state. The

\* Research sponsored by Grant No. 4624 from the National Research Council of Canada.

† Holder of National Research Council of Canada Scholarship 1968-69.

<sup>1</sup> C. P. Slichter, *Phys. Rev.* **99**, 479 (1955).

<sup>2</sup> G. Feher, R. C. Fletcher, and E. A. Gere, *Phys. Rev.* **100**, 1784 (1955).

<sup>3</sup> J. R. Marko, *Phys. Letters* **27A**, 119 (1968).

<sup>4</sup> G. Feher and E. A. Gere, *Phys. Rev.* **114**, 1245 (1959).

<sup>5</sup> A. Honig, in *Quantum Electronics*, edited by C. H. Townes (Columbia University Press, New York, 1960), p. 450.

energy levels in this case are written simply as

$$E_T^{(0),(\pm 1)} = g\mu_B H_0 M + \frac{1}{2} A M (m_1 + m_2) + \frac{1}{4} J \quad (3)$$

and

$$E_s = -\frac{3}{4} J, \quad (4)$$

where the subscripts  $T$  and  $S$  refer to the electronic spin triplet and single states, respectively, and the superscripts on  $E_T$  refer to the  $z$  component of the total electronic spin of the pair  $M$ . Since it has been shown<sup>6</sup> that  $J > 0$ , the more energetic (for  $J > g\mu_B H_0 + \frac{1}{2} A$ ) magnetic triplet states can become thermally depopulated at low temperatures.

It can be seen that a perturbation of the form

$$\mathcal{H}_{rf} = g\mu_B H_1 (S_{1x} + S_{2x}) \sin \omega t, \quad (5)$$

representing the microwave field of intensity  $H_1$  and angular frequency  $\omega$  used in the observation of EPR, will have no non-negligible matrix elements connecting the electronic spin singlet and triplet states when  $J \gg A$ . The resultant selection rule prohibiting the corresponding transitions arises from the fact that, under such conditions, the electronic spin interchange operator commutes with the Hamiltonian giving a definite parity to the energy eigenstates. As a result,  $\mathcal{H}_{rf}$ , which is symmetric or, in other words, unchanged by an interchange of spins 1 and 2, cannot connect the singlet and triplet states which have opposite parity under the interchange. Applying these selection rules [ $\Delta S = 0$ ,  $\Delta M = \pm 1$ , and  $\Delta(m_1 + m_2) = 0$ ] to the triplet energy levels of Eq. (3), we find "allowed" lines at the energies  $g\mu_B H_0 \pm \frac{1}{2} A$  and one of double intensity (due to two possible degenerate nuclear spin states) at  $g\mu_B H_0$ . These are the so-called "pair lines."<sup>11</sup> No electronic spin transitions involving the singlet state are allowed when  $J \gg A$ .

Similarly, if we consider pairs such that  $m_1 = m_2$ , it is obvious that interchange of the two electronic spins will leave the energy of the pair unchanged, leading again to the above selection rules for all values of  $J$ .

However, if  $m_1 \neq m_2$  and  $J/A$  is no longer  $\gg 1$ , interchange of the two electronic spins does not leave the energy unchanged [the spin interchange does not commute with Eq. (1)], and the electronic spin states no longer have a definite parity under such an operation. This, in effect, mixes the singlet and triplet states and leads to a spectrum significantly different from that in the  $J/A \gg 1$  limit.

Our calculation diagonalizes Eq. (1), retaining only the diagonal portion of the hyperfine interaction,  $A(I_{1z}S_{1z} + I_{2z}S_{2z})$ , using direct product basis functions of the form  $|M_1, M_2, m_1, m_2\rangle$ , where  $M_i$  and  $m_i$  correspond to the  $z$  component of the electronic and nuclear spin, respectively, of the  $i$ th donor of a pair. In addition, we require the resultant eigenfunctions to have a definite parity under simultaneous interchange of both the electronic and nuclear spins. This stipulation arises because such an interchange leaves the energy unchanged and commutes with the Hamiltonian for all values of  $J$ .

<sup>6</sup> D. Jerome and J. M. Winter, Phys. Rev. 134, A1001 (1964).

STATE NO.	STATE	ENERGY
1	$ T_1, t_1\rangle$	$\gamma_e + \frac{J}{4} + \frac{A}{2}$
2 & 3	$ T_1, t_0\rangle,  T_1, s\rangle$	$\gamma_e + \frac{J}{4}$
4	$ T_1, t_{-1}\rangle$	$\gamma_e + \frac{J}{4} - \frac{A}{2}$
5 & 9	$ T_0, t_1\rangle,  T_0, t_{-1}\rangle$	$\frac{J}{4}$
7 & 8	$ T_0, t_0\rangle,  T_0, s\rangle$	$-\frac{J}{4} + \frac{1}{2} \sqrt{J^2 + A^2}$
16	$ T_{-1}, t_{-1}\rangle$	$-\gamma_e + \frac{J}{4} + \frac{A}{2}$
14 & 15	$ T_{-1}, t_0\rangle,  T_{-1}, s\rangle$	$-\gamma_e + \frac{J}{4}$
13	$ T_{-1}, t_1\rangle$	$-\gamma_e + \frac{J}{4} - \frac{A}{2}$
6 & 10	$ S, t_1\rangle,  S, t_{-1}\rangle$	$-\frac{3J}{4}$
11 & 12	$ S, t_0\rangle,  S, s\rangle$	$-\frac{J}{4} - \frac{1}{2} \sqrt{J^2 + A^2}$

FIG. 1. Energy-level diagram for a phosphorus donor pair. The eigenstates are labeled numerically from 1 to 16 along with the usual strongly coupled pair states (Ref. 6) to which each reduces in the limit  $J/A \gg 1$ . The eigenvalues of the spin Hamiltonian are given using the notation  $\nu_e = g\mu_B H_0$ .

In Fig. 1, we have presented graphically the energy levels arising from such a diagonalization. The corresponding eigenstates are labeled from (1) to (16) together with the strongly coupled state to which each reduces in the  $J/A \gg 1$  limit. The notation for these strongly coupled states is similar to that of Jerome and Winter<sup>6</sup> where  $S$ ,  $T_0$ , and  $T_{\pm 1}$  refer to electronic pair spin states and  $s$ ,  $t_0$ , and  $t_{\pm 1}$  refer to similar pair nuclear spin states.

By taking the square of the matrix elements of  $\mathcal{H}_{rf}$  between any two of these eigenstates, the relative intensities of the corresponding transitions were calculated. These relative intensities (normalized to transition  $a$ ) and corresponding energies are listed in Table I for all not completely forbidden transitions. Here again, it is seen that the usual pair spectrum, with conservation of total electronic spin, appears both in the strong coupling limit and in pairs where  $m_1 = m_2$ . The latter result is evident in the fact that the only transitions linking states where  $m_1 = m_2$  (transitions  $a$ ,  $b$ ,  $c$ , and  $d$ ) occur at the energies  $g\mu_B H_0 \pm \frac{1}{2} A$  and with the probabilities predicted by a simple application of  $\mathcal{H}_{rf}$  to the ( $S=1$ ) spin triplet.

The last eight transitions listed in Table I involve states where  $m_1 \neq m_2$ . In these cases, at low values of

TABLE I. Donor pair transitions having nonzero transition probability. The relative transition probabilities and the transition energies  $\Delta$  are given and  $\nu_e = g\mu_B H_0$ .

Transition	Relative transition probability	Transition energy ( $\Delta$ )
$a: (16) \leftrightarrow (9)$	1	$\nu_e - \frac{1}{2}A$
$b: (13) \leftrightarrow (5)$	1	$\nu_e + \frac{1}{2}A$
$c: (9) \leftrightarrow (4)$	1	$\nu_e - \frac{1}{2}A$
$d: (5) \leftrightarrow (1)$	1	$\nu_e + \frac{1}{2}A$
$e: (15) \leftrightarrow (8)$	$\frac{1}{2}[1 + J(J^2 + A^2)^{-1/2}]$	$\nu_e + \frac{1}{2}(J^2 + A^2)^{1/2} - \frac{1}{2}J$
$f: (14) \leftrightarrow (7)$	$\frac{1}{2}[1 + J(J^2 + A^2)^{-1/2}]$	$\nu_e + \frac{1}{2}(J^2 + A^2)^{1/2} - \frac{1}{2}J$
$g: (8) \leftrightarrow (3)$	$\frac{1}{2}[1 + J(J^2 + A^2)^{-1/2}]$	$\nu_e - \frac{1}{2}(J^2 + A^2)^{1/2} + \frac{1}{2}J$
$h: (7) \leftrightarrow (2)$	$\frac{1}{2}[1 + J(J^2 + A^2)^{-1/2}]$	$\nu_e - \frac{1}{2}(J^2 + A^2)^{1/2} + \frac{1}{2}J$
$i: (15) \leftrightarrow (11)$	$\frac{1}{2}[1 - J(J^2 + A^2)^{-1/2}]$	$\nu_e - \frac{1}{2}(J^2 + A^2)^{1/2} + \frac{1}{2}J$
$j: (14) \leftrightarrow (12)$	$\frac{1}{2}[1 - J(J^2 + A^2)^{-1/2}]$	$\nu_e - \frac{1}{2}(J^2 + A^2)^{1/2} + \frac{1}{2}J$
$k: (12) \leftrightarrow (2)$	$\frac{1}{2}[1 - J(J^2 + A^2)^{-1/2}]$	$\nu_e + \frac{1}{2}(J^2 + A^2)^{1/2} + \frac{1}{2}J$
$l: (11) \leftrightarrow (3)$	$\frac{1}{2}[1 - J(J^2 + A^2)^{-1/2}]$	$\nu_e + \frac{1}{2}(J^2 + A^2)^{1/2} + \frac{1}{2}J$

$J$ , the results deviate significantly from those of the strong coupling limit. For example, the "central-pair line," at low values of  $J$ , splits into a component (transitions  $e, f$ ) at an energy  $\frac{1}{2}(J^2 + A^2)^{1/2} - \frac{1}{2}J$  above  $g\mu_B H_0$  and a component (transitions  $g, h$ ) at  $g\mu_B H_0 - [\frac{1}{2}(J^2 + A^2)^{1/2} - \frac{1}{2}J]$ . In addition, widely split "satellite" lines appear outside the usual isolated donor "hyperfine" lines at  $g\mu_B H_0 \mp [\frac{1}{2}J + \frac{1}{2}(J^2 + A^2)^{1/2}]$  (transitions  $i, j, k$ , and  $l$ ). As expected, all of these lines reduce to give the two "hyperfine" line spectra of isolated donors as  $J$  approaches zero. While, in the strong coupling limit, the probability for the satellite lines vanishes and the remaining ( $e, f, g$ , and  $h$ ) transitions coalesce to give the usual central-pair line.<sup>3</sup>

The calculations discussed thus far have been concerned with the spectrum of a pair having a given exchange energy  $J$ . The observed EPR signal will be a summation of these individual spectra over the quasi-continuous range of  $J$  values made possible for pairs by the random placement of donors in the host lattice. This random impurity assumption has so far appeared to be valid in other work involving similar samples.<sup>7</sup> Using this assumption, and that of a continuous distribution of impurity positions, Chandrasekhar<sup>8</sup> has derived an expression for  $W(R)dR$ , the probability that a nearest-neighbor donor exists in the volume of an imaginary spherical shell of radius  $R$  and thickness  $dR$  centered on a given first donor atom. This probability for a sample with  $N_0$  donors/(unit volume), can be written as

$$W(R)dR = (e^{-4\pi R^3 N_0/3})(4\pi N_0 R^2 dR). \quad (6)$$

The first term in parentheses on the right-hand side of this expression represents the total probability that all positions at separations less than  $R$ , from the central donor, are not occupied by a donor; while the second

factor corresponds to the probability that a donor exists in the shell of radius  $R$ .

The treatment in this paper assumes that the net EPR spectrum of the  $N_0$  donors/(unit volume) is describable in terms of  $\frac{1}{2}N_0$  nearest-neighbor pairs. The distribution of pair separations in a unit volume  $N(R)dR$  is obviously obtained from expression (6) as

$$N(R)dR = \frac{1}{2}N_0(e^{-4\pi R^3 N_0/3})(4\pi N_0 R^2 dR). \quad (7)$$

This grouping of the donors into pairs is done even though members of the large fraction of these "pairs," having very small  $J$ , will act as isolated donors. As it should be, the spectrum of such pairs, on the basis of the above calculation, becomes identical to that of isolated donors. As pointed out elsewhere,<sup>9</sup> certain difficulties do arise from such classification into pairs. For example, the nearest neighbor of atom "A" may be atom "B" whose nearest neighbor is, however, atom "C." Classification into pairs using expression (7) under such circumstances is ambiguous and, in fact, requires more detailed treatment. However, for the donor concentration considered here ( $\leq 3.7 \times 10^{16}$  donors/cm<sup>3</sup>), such ambiguities arise primarily in those pairs having very large donor separations.<sup>9</sup> Because of the very small  $J$  values of such pairs, their spectrum is essentially independent of  $J$  and effectively identical to that of completely isolated donors. Consequently, errors in the calculated EPR spectrum arising from such cases are negligible for the sample concentrations considered. The absence of the well-known spectra of three and four donor atoms in our experiments similarly justifies our neglect of these multiple couplings in the calculations for such concentrations.

Thus, considering the donor spins to be a collection of nearest-neighbor pairs, expression (7) can be used to obtain the distribution of  $J$  values,  $N(J)$ , in a given sample if we have available an expression  $J(\mathbf{R})$  relating the exchange energy of a pair to the displacement vector  $\mathbf{R}$  connecting its two donors. In obtaining such an expression, we have adapted a general expression for the exchange energy of two electrons in an attractive potential<sup>10</sup> into the following form:

$$J = -2 \int \psi_i^*(\mathbf{r}_1) \psi_j(\mathbf{r}_1) \int \psi_j^*(\mathbf{r}_2) V(\mathbf{r}_2) \psi_i(\mathbf{r}_2) d\mathbf{r}_1 d\mathbf{r}_2 - \int \psi_i^*(\mathbf{r}_1) \psi_j(\mathbf{r}_1) \frac{e^2}{K_0 |\mathbf{r}_1 - \mathbf{r}_2|} \psi_j^*(\mathbf{r}_2) \psi_i(\mathbf{r}_2) d\mathbf{r}_1 d\mathbf{r}_2, \quad (8)$$

where  $\psi_i$  and  $\psi_j$  refer to wave functions centered on the two donor nuclei of the pair ( $i$  and  $j$ ),  $\mathbf{r}_1$  and  $\mathbf{r}_2$  refer to the spatial coordinates of the two donor electrons,  $K_0 = 12$  is the dielectric constant of silicon, and  $V(\mathbf{r}_2)$  represents the attractive potential of the donor nucleus. Following the approach of Jerome and Winter,<sup>6</sup> we have

<sup>7</sup> M. N. Alexander and D. F. Holcomb, Rev. Mod. Phys. **40**, 815 (1968).

<sup>8</sup> S. Chandrasekhar, Rev. Mod. Phys. **15**, 1 (1943).

<sup>9</sup> E. Sonder and H. C. Schweinler, Phys. Rev. **117**, 1216 (1960).

<sup>10</sup> P. W. Anderson, in *Solid State Physics*, edited by F. Seitz and D. Turnbull (Academic Press Inc., New York, 1963), Vol. 14.

expressed  $\psi_i$  and  $\psi_j$  in terms of the Kohn-Luttinger donor wave functions<sup>11</sup> which are of the form

$$\psi(\mathbf{r}) = \sum_{j=1}^{j=6} F^j(\mathbf{r})\phi_j(\mathbf{r}), \quad (9)$$

where  $\phi_j(\mathbf{r})$  is the Bloch function associated with the  $j$ th of the six conduction-band minima of silicon and  $F^j(\mathbf{r})$  is a hydrogenic envelope function in which the effective mass at each of these minima has been assumed to be isotropic. This latter assumption neglects the observed anisotropy but simplifies the calculations greatly, since the envelope function can now be written as

$$F^j(\mathbf{r}) = (\pi a^*)^{-3/2} e^{-|\mathbf{r}|/a^*}, \quad (10)$$

where  $a^*$  is the effective Bohr radius of the donor electron.

Following the substitution of Eqs. (9) and (10) into expression (8) and the subsequent evaluation of the resulting integrals through the use of the earlier results of Miller and Abrahams,<sup>12</sup> we have obtained the following expression for the exchange energy of a pair having a separation vector  $\mathbf{R}$ :

$$\begin{aligned} J(\mathbf{R}) = & (e^2/K_0 a^*) \{ (2/9)(1+D)(1+D+\frac{1}{3}D^2)e^{-2D} \\ & - (1/45)[(25/8 - (23/4)D - 3D^2 - \frac{1}{3}D^3) \\ & + (6/D)(1+D+\frac{1}{3}D^2)(\gamma + \ln D)]e^{-2D} \\ & - (1-D+\frac{1}{3}D^2)^2 E_i(-4D)e^{2D} \\ & + 2(1+D+\frac{1}{3}D^2)(1-D+\frac{1}{3}D^2)E_i(-2D) \} \\ & \times (\sum_{j=1,2,3} \cos \mathbf{k}_j \cdot \mathbf{R}), \quad (11) \end{aligned}$$

where

$$D = |\mathbf{R}|/a^*, \quad \gamma = 0.57722, \quad \text{Ei}(-x) = - \int_x^\infty \frac{e^{-t}}{t} dt,$$

and the  $\mathbf{k}_j = 0.85\mathbf{k}_{j\max}$  represent the values of the wave vectors at the conduction-band minima in three mutually perpendicular [100] directions. It is important to note the strong directional dependence of  $J$  upon  $\mathbf{R}$  introduced by the squared sum of cosines factor of Eq. (11). This dependence comes from the interference between those portions of the wave-function equation (9) which arise from different conduction-band "valleys." This interference factor has been omitted both from the results of Jerome and Winter<sup>6,13</sup> and the earlier evaluation of the second term of expression (8) by Miller and Abrahams.<sup>12</sup> The interference factor has been retained in the present calculation. Before going into the details of this calculation it should be emphasized that  $a^*$ , the effective Bohr radius, will be regarded as the sole adjustable parameter in expression (11) and

it is our purpose to determine its value through a comparison of calculated and experimental results.

Because of the directional dependence of expression (11), a more complete calculation required a consideration of the discrete silicon lattice and thus the finite set of values available for  $\mathbf{R}$ . In this case, the probability of a nearest-neighbor donor occupying a site of separation vector  $\mathbf{R}$  can be written as

$$W(\mathbf{R}) = (e^{-4\pi N_0 |\mathbf{R}|^3/3}) (N_0/N_{\text{Si}}), \quad (12)$$

where  $N_{\text{Si}}$  represents the number of silicon lattice sites per unit volume. This expression differs from the earlier expression (7) primarily in that the probability of donor occupancy of the given lattice site is now presented by  $N_0/N_{\text{Si}}$ . The retention in (12) of the first factor of expression (6) which represents the probability that all sites interior to  $\mathbf{R}$  are vacant of donors, is an approximation which is valid for all but the smallest values of  $\mathbf{R}$ . The statistical weight of these small  $\mathbf{R}$  pairs is so small that this approximation has negligible effect on our results.  $N(J)$  is then obtained by computing the sum

$$N(J) = \frac{1}{2} N_0 \sum_{\mathbf{R}'} W(\mathbf{R}'), \quad (13)$$

where  $\mathbf{R}'$  represents all those sites for which expression (11) yields a value equal to  $J$ .

Given the distribution  $N(J)$ , further spectral calculations require the assumption of thermal equilibrium at the bath temperature  $T$ . The population differences between the various states involved in the transitions of Table I are taken into account by assigning a thermal weighting factor of unity to state (12) of Fig. 1 while letting that of the  $i$ th state be  $e^{-(E_i - E_{12})/kT}$ . Together with the relative transition probabilities calculated earlier, this gives a relative, rather than absolute, value for the EPR intensity at given energy  $\Delta$ . This is sufficient since our experiment measures only such relative intensities, as calibration for absolute measurements has been found unnecessary.

Finally, our calculation allows for the inhomogeneous broadening of each transition into a Gaussian line shape of half-width (in frequency units) of 8.0 MHz by the nuclear magnetic moment of the Si<sup>29</sup> isotope present in the host lattice.<sup>14</sup> The resultant spectrum is calculated by performing a computer sum over all pairs having transitions at the various energies  $\Delta$ , using the corresponding transition probabilities of Table I, with  $N(J)$  obtained as above, and with the obvious allowances for the population weighting factor and Gaussian line shape. The resultant calculated spectrum is a function of temperature, concentration, and the effective donor radius  $a^*$ . However, because of the previously mentioned restrictions to relatively dilute concentrations, we are confined experimentally to samples where the "broad background" portion of the EPR signal is so weak as to preclude its detailed study by direct tech-

<sup>11</sup> W. Kohn, in Ref. 10, Vol. 5.

<sup>12</sup> A. Miller and E. Abrahams, Phys. Rev. **120**, 745 (1960).

<sup>13</sup> D. Jerome, Ph.D. thesis, University of Paris, 1965 (unpublished).

<sup>14</sup> G. Feher, Phys. Rev. **114**, 1219 (1959).

niques. For this reason, in connection with our determination of the exchange energy  $J$ , it is sufficient to calculate the ratio of the signal height at the "central-pair line" peak ( $\Delta = g\mu_B H_0$ ) to that at either "hyperfine line" ( $\Delta = g\mu_B H_0 \pm \frac{1}{2}A$ ). This ratio is easy to determine experimentally as a function of concentration and temperature. In Sec. III, we shall discuss such experiments and the subsequent matching with the calculated results.

### III. EXPERIMENTS AND RESULTS

The EPR spectra were obtained for four samples of phosphorus-doped silicon having negligible acceptor impurity concentration and having donor concentrations of 0.8, 1.7, 2.3, and  $3.7 \times 10^{16}$  donors/cm<sup>3</sup>. A standard  $x$ -band spectrometer with 400-Hz magnetic field modulation was used. The klystron frequency was locked to an external wavemeter cavity to enable observation in the dispersive mode. Temperatures ranging from 1.05 to 4.2°K were available through controlled pumping on a liquid-helium-4 bath.

The results of these measurements, at  $T = 1.05^\circ\text{K}$ , of  $C$ , the ratio of the central-pair to hyperfine line intensity, are plotted in Fig. 2 as a function of the donor concentration. The results represented by the solid curve in this figure were calculated on the basis of the theoretical spectrum of Sec. II and an assumed effective Bohr radius  $a^* = 17.3 \text{ \AA}$ . This value of  $a^*$  gives the best fit to all experimental data.

The error brackets on the experimental points of Fig. 2 reflect both the limitations of our intensity measurements and a possible  $\sim \pm 5\%$  error in our concentration determinations made through the use of a standard four-point probe resistivity technique. An additional error could arise from the existence of different EPR signal passage conditions for the fast

relaxing pairs relative to the slower small exchange-energy pairs.<sup>15</sup> To check this possibility, several parameters of the observation mode were varied in the measurements. In particular, the magnetic field modulation frequency was varied from 30 to 3000 Hz, and several magnetic field sweep rates were used. Within experimental error,  $C$  was found to be independent of these changes in the observation parameters.

It is also important to note that care must be taken to keep the microwave power used in signal observation at its lowest possible value consistent with a useable signal to noise ratio. This precaution was necessary since the value obtained for  $C$  was found to increase at high powers, most likely due to the broad saturation effect reported earlier.<sup>3</sup> In this effect, off-resonant microwave power was observed to reduce the size of the hyperfine lines, presumably through spectral diffusion from the saturated portion of the broad background line. In the present case, the faster relaxing central line would be less affected by this process than the more slowly relaxing hyperfine lines, thus yielding a larger ratio  $C$  at higher power levels.

On the basis of our exchange-energy determination, the temperature dependence of the ratio  $C$  was calculated. The predicted value at 4.2°K was  $C = 20.2\%$ , for a  $3.7 \times 10^{16}$  donors/cm<sup>3</sup> sample, which was in reasonable agreement with our measured value of  $C = (20 \pm 2)\%$ .

In estimating the maximum error possible in our determination, we have calculated the values of  $a^*$  necessary to match the experimental points at the limits of the error brackets of Fig. 2. The resultant possible error is  $\pm 0.2 \text{ \AA}$ .

### IV. DISCUSSION

The experimentally determined value of the effective Bohr radius,  $a^* = 17.3 \text{ \AA}$ , is very close to the  $17.2 \text{ \AA}$

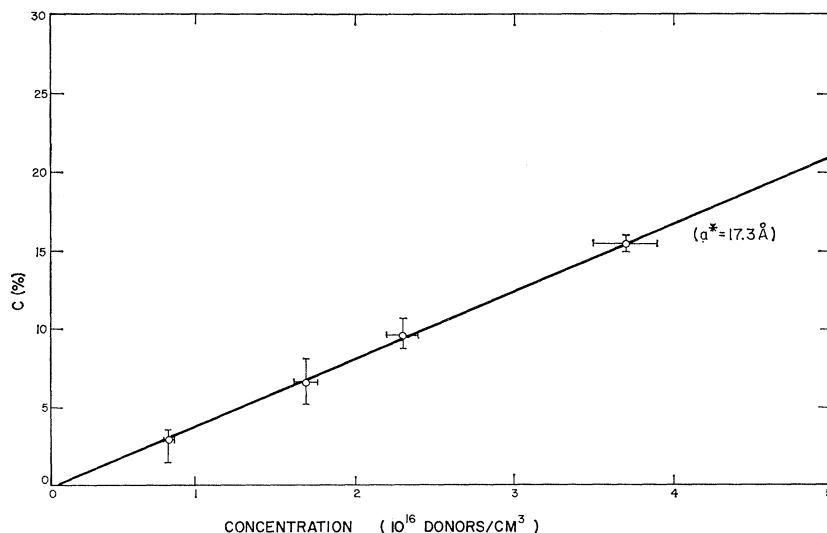


FIG. 2. Plot of experimental points and theoretically calculated values of the ratio  $C$  (%) of the central-pair line ( $\Delta = g\mu_B H_0$ ) to intensity to that of either hyperfine line ( $\Delta = g\mu_B H_0 \pm \frac{1}{2}A$ ). The solid curve represents the calculated ratio for an effective Bohr radius  $a^* = 17.3 \text{ \AA}$ .

<sup>15</sup> G. Yang and A. Honig, Phys. Rev. **168**, 271 (1967).

value obtained for the arithmetic mean of the three previously estimated components of the anisotropic donor radius.<sup>12</sup> These latter values were derived from optical and thermal data interpreted through corrections applied to the effective-mass formalism.<sup>11</sup> The agreement obtained in our work would seem to indicate that, at least in overlap calculations, the effective Bohr radius of isotropic envelope wave functions should be set equal to such an arithmetic mean radius. This has not been done in previous calculations.<sup>16</sup>

The errors introduced by the assumption of an isotropic effective Bohr radius, while obviously important in determining the accuracy with which the theoretical donor wave functions describe the physical situation, should not greatly affect the resultant exchange-energy distribution. The experimentally determined normalized distribution  $N(J)/\frac{1}{2}N_0$ , for samples of concentrations  $N_0 = 4 \times 10^{16}$  and  $6 \times 10^{16}$  donors/cm<sup>3</sup>, are plotted in Fig. 3. Of course, since the exchange-energy distribution is not continuous, the plotted curves represent suitable averages of the discrete  $J$ -value distribution.

We should now like to compare certain features of these exchange-energy distributions with the corresponding results of earlier experiments in this material. In particular, our results indicate that the peak of the distribution function  $N(J)$  for a  $6 \times 10^{16}$ -donors/cm<sup>3</sup> sample, occurs at  $J \sim 50$  MHz. This value is much lower than the previous estimate<sup>6</sup> of  $1.35 \times 10^4$  MHz made from ENDOR experiments. Part of this discrepancy is due to the severe complications introduced into the interpretation of the ENDOR experiments by the  $J$  dependence of the pair electronic and nuclear spin-lattice relaxation times. In addition, these latter experiments involved only the more strongly coupled pairs having exchange energies greater than a few hundred MHz. For these reasons, we feel that the details of the exchange-energy distribution obtainable from ENDOR experiments are quite limited.

Maekawa and Kinoshita,<sup>17</sup> by measuring the temperature dependence of the central-pair line intensity, have estimated the average  $J$  value for those pairs contributing to this line to be  $8 \times 10^3$  MHz for a  $4 \times 10^{16}$ -donors/cm<sup>3</sup> sample. This is greater, by a factor of  $\sim 5$ , than a similar quantity obtained from our results. Such a discrepancy can be accounted for by large possible experimental errors, ambiguity in the definition of the average exchange energy, and the fact that the earlier work separated out the central-pair and background lines and treated them independently. As a result, we feel that our unified treatment and direct spectral measurements offer the more reliable information on the distribution of exchange energies.

In conclusion, it appears that the excellent agreement between the calculated and experimental results pro-

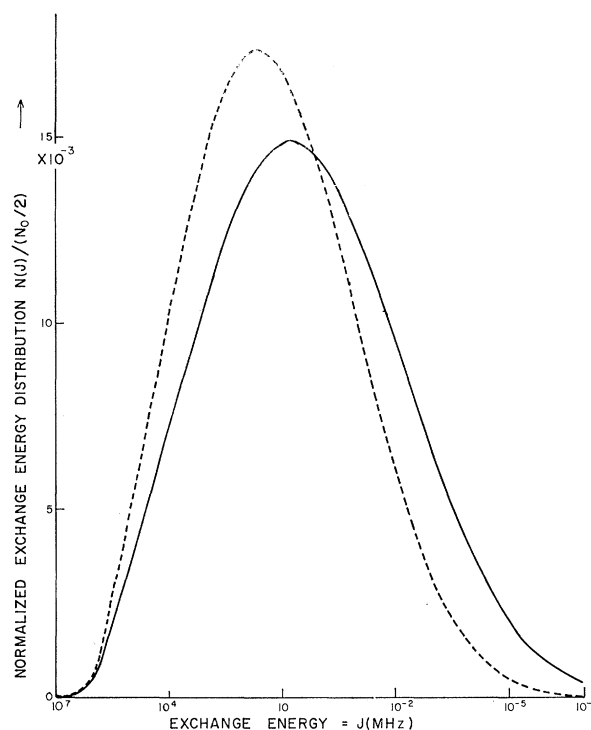


FIG. 3. A plot of the normalized distribution of pair  $J$  values,  $N(J)/\frac{1}{2}N_0$ , as a function of the exchange energy  $J$  for a  $4 \times 10^{16}$ -donors/cm<sup>3</sup> sample (solid curve) and a  $6 \times 10^{16}$ -donors/cm<sup>3</sup> sample (dashed curve).

vides strong support for the assumption of a random impurity distribution and for the reasonable accuracy with which expression (11) with  $a^* = 17.3$  Å represents the exchange energy of a donor pair. The closeness of this value of  $a^*$  to the arithmetic mean of the three anisotropic donor radii determined elsewhere<sup>12</sup> indicates the correctness of the use of this latter quantity in similar calculations requiring the simplification of isotropic envelope functions. The exchange-energy distribution resultant from the present calculation should be useful in extensions of such spectrum calculations to higher concentrations where larger donor clusters must be considered as well as in a detailed study of the so-called concentration-dependent spin-lattice relaxation processes.<sup>18</sup>

#### ACKNOWLEDGMENT

We would like to acknowledge the generous cooperation of Professor A. Honig and M. Davidoff of Syracuse University in providing us with additional samples for cross checking our concentration-determination measurements. In addition, one of us (J. R. M.) would like to acknowledge useful discussions with Professor R. Barrie and Professor S. Alexander of the University of British Columbia, and Professor A. Miller of Syracuse University.

<sup>18</sup> J. R. Marko and A. Honig (to be published).

<sup>16</sup> K. Sugihara, J. Phys. Chem. Solids **29**, 1099 (1968).

<sup>17</sup> S. Maekawa and N. Kinoshita, J. Phys. Soc. Japan **20**, 1447 (1965).